PROCEEDINGS OF SCIENCE

Direct CP violation and the $\Delta I = 1/2$ rule in $K \to \pi\pi$ decay in the Standard Model

Christopher Kelly[a,*]

[a] *Computational Science Institute, Brookhaven National Laboratory, Upton, New York, USA.*

E-mail: ckelly@bnl.gov

We discuss the RBC & UKQCD collaborations' recent [1] lattice calculation of ϵ', the measure of direct CP-violation in kaon decays. This result significantly improves on our previous 2015 calculation, with nearly 4× the statistics and more reliable systematic error estimates. We discuss how our results demonstrate the Standard Model origin of the $\Delta I = 1/2$ rule, and present our plans for future calculations.

The 38th International Symposium on Lattice Field Theory, LATTICE2021 26th-30th July, 2021 Zoom/Gather@Massachusetts Institute of Technology

*Speaker

PoS(LATTICE2021)008

1. Introduction

CP-violating (CPV) processes provide very sensitive probes for new physics as they are highly suppressed in the Standard Model. New sources of CPV beyond the Standard Model appear to be necessary if the matter-antimatter asymmetry in the Universe is explained by baryogenesis, which requires CPV at a level much higher than predicted by the Standard Model according to current best estimates. Direct CP-violation in kaon decays is particularly strongly suppressed, and as a result was only observed comparatively recently – in the late-1990s – by the NA48 [2] and KTeV [3] experiments in the decay of neutral kaons into two pions. The current world average of the measure of direct CPV in $K \to \pi\pi$ decays, ϵ', is [4]

$$\mathrm{Re}(\epsilon'/\epsilon) = 16.6(2.3) \times 10^{-4} \tag{1}$$

where ϵ is the measure of indirect CP-violation, itself heavily suppressed: $|\epsilon| = 2.228(11) \times 10^{-3}$.

In order to take advantage of this precise experimental result, a correspondingly precise Standard Model prediction is necessary. Unfortunately, while the underlying physics occurs at the weak interaction scale, $O(80)$ GeV, these processes receive large corrections from low-energy non-perturbative physics at the $O(250)$ MeV hadronic energy scale, hence it was only recently that a reliable first-principles calculation of ϵ' has been performed [5]. This 2015 calculation was performed by the RBC & UKQCD collaborations using lattice QCD, the only known *ab initio* and systematically improvable method – one for which all of the systematic errors can be identified and improved and/or eliminated with sufficient computational expense – for computing non-perturbative processes. The value obtained,

$$\mathrm{Re}(\epsilon'/\epsilon) = 1.38(5.15)(4.59) \times 10^{-4} \tag{2}$$

where the errors are statistical and systematic respectively, is 2.1σ below the experimental value. Spurred by the hint of a tension between the lattice prediction and the experimental number and an unexplained discrepancy between the predicted value of the $I = 0$ $\pi\pi$ scattering phase shift at the kaon mass (a necessary component of the calculation) and the dispersive prediction, we have since endeavored to improve our calculation by significantly increasing the statistics, incorporating more sophisticated techniques for removing excited state systematic effects in our matrix element fits, and also to reduce our dependence on perturbation theory at low energies in the matrix element renormalization. As a result of this effort we have now resolved the discrepancy in the $\pi\pi$ phase shift and have produced a new value with a factor of two smaller statistical errors and more reliable systematic error estimates [1]:

$$\mathrm{Re}(\epsilon'/\epsilon) = 21.7(2.6)(6.2)(5.0) \times 10^{-4}\,. \tag{3}$$

Here the third error quoted is an estimate of the effects of isospin-breaking and electromagnetism. This result is now in good agreement with the experimental number.

In this document we summarize the techniques and measurements that comprise this most recent calculation and discuss the results in more detail, and then follow this by a description of our current efforts and future plans for further improving the calculation.

2. Calculation overview

The lattice calculations are performed with degenerate up and down quarks, resulting in an isospin-symmetric theory in which ϵ' can be expressed directly in terms of the difference in the complex phases of A_0 and A_2, the amplitudes of neutral kaons decaying into $\pi\pi$ states of isospin $I = 0$ ($\Delta I = 1/2$) and $I = 2$ ($\Delta I = 3/2$), respectively,

$$\epsilon' = \frac{i\omega e^{i(\delta_2 - \delta_0)}}{\sqrt{2}} \left(\frac{\mathrm{Im}A_2}{\mathrm{Re}A_2} - \frac{\mathrm{Im}A_0}{\mathrm{Re}A_0} \right), \tag{4}$$

where $\omega = \mathrm{Re}A_2/\mathrm{Re}A_0$ and δ_I are the $\pi\pi$ scattering phase shifts. We work in three-flavor QCD (i.e. without a charm quark), in which the underlying weak interaction Hamiltonian is expressed to first order in the weak effective theory as a series of ten four-quark operators Q_i and the corresponding Wilson coefficients z_i, y_i that encapsulate the high-energy contributions:

$$H_W = \frac{G_F}{\sqrt{2}} V_{ud}^* V_{us} \sum_{i=0}^{10} [z_i(\mu) + \tau y_i(\mu)] Q_i(\mu) \tag{5}$$

where $\tau = -\frac{V_{ts}^* V_{td}}{V_{us}^* V_{ud}}$ and the scale μ indicates that the Wilson coefficients and operator are renormalization scheme dependent (while their product is not). The lattice calculation requires evaluating this effective Hamiltonian between a kaon initial state and a two-pion final state in the appropriate isospin representation:

$$A^I = \langle (\pi\pi)_I | H_W | K^0 \rangle \,. \tag{6}$$

Aside from the usual difficulties of performing a lattice calculation – tuning ensembles and operators, gathering sufficient statistics, etc – the evaluation of these matrix elements involves a number of additional challenges:

1. On a conventional lattice, the three-point functions from which the matrix elements are extracted by fitting the large-time behavior, are dominated by an unphysical, energy non-conserving decay amplitude between a kaon of mass ∼500 MeV and two pions at rest with an energy of ∼260 MeV. It is therefore necessary to either attempt to extract a subdominant contribution from already noisy data, or to exploit some other technique to remove this unphysical contribution. We discuss this in more detail below.

2. Due to the compression of the two-pion final state by the finite box size, these matrix elements obtain substantial finite-volume corrections. Fortunately, the dominant, power-law component of this correction can be computed very precisely in the form of the Lellouch-Lüscher factor [6] F, leaving only small, exponentially-suppressed contributions as a remaining systematic error. The computation of F requires knowledge of the derivative of the $\pi\pi$ phase shift with respect to energy which must be either computed on the lattice or obtained from the dispersive analysis of experimental data.

3. The bare lattice matrix elements are divergent and must be renormalized (into the same scheme as the Wilson coefficients) prior to removing the lattice cutoff. Unfortunately the $\overline{\mathrm{MS}}$ scheme in which the Wilson coefficients are conventionally computed is not amenable to a non-perturbative treatment on the lattice, hence we must first renormalize into an intermediate

non-perturbative renormalization (NPR) scheme – in our case the regularization-invariant momentum schemes (RI-SMOM) – before matching perturbatively to $\overline{\text{MS}}$. In order to avoid large perturbative truncation effects it is necessary to perform this matching at as high of a scale as possible while maintaining sufficient separation from the lattice cutoff to avoid discretization effects.

The calculation of the $I = 0$ amplitude introduces further complexities:

1. Some of the the diagrams entering this amplitude contain loops in which two of the legs of the four-quark operator contract together, resulting in a quadratic divergence regulated by the lattice cutoff. While this divergence is not present in the case of exactly energy conserving kinematics, in practise this condition can only be achieved approximately through careful tuning, and therefore it is advantageous to remove it directly by defining subtracted operators

$$Q_i \to Q_i - \alpha_i \bar{s}\gamma^5 d \tag{7}$$

where the coefficients α_i are defined through a suitable condition:

$$\langle 0|\left\{Q_i(t) - \alpha_i(t)[\bar{s}\gamma^5 d](t)\right\} O_K(0)|0\rangle = 0\,, \tag{8}$$

where $O_K(0)$ is an operator that creates an incoming kaon state. This subtraction offers the additional benefit of suppressing excited state matrix elements that would otherwise be enhanced by their non-energy conserving kinematics even if the primary matrix element of interest were exactly energy conserving.

2. The $I = 0$ final state has vacuum quantum numbers, hence we must perform an explicit subtraction to remove the contribution of the vacuum intermediate state. The vacuum quantum numbers also mean that it is necessary to evaluate disconnected diagrams, which are typically very noisy and therefore require advanced methods and large statistics to achieve a good signal.

3. $I = 2$ calculation

The $\Delta I = 3/2$ decay is generated by three linear combinations of Q_i that are conventionally labeled by their transformation properties under chiral $SU(3)_L \times SU(3)_R$: the $(27, 1)$ combination is the domininant contribution to $\text{Re}A_2$, and the $(8, 8)$ and $(8, 8)_{\text{mx}}$, where mx indicates the operator is color-mixed, are the domininant contributions to $\text{Im}A_2$. The measurement of A_2 was first performed by the RBC & UKQCD collaborations in 2012 [7, 8] on a single lattice with physical pion masses and a somewhat coarse inverse lattice spacing of $a^{-1} = 1.378(7)$ GeV, but with a correspondingly large physical volume to offer good control over residual finite-volume effects. This was later followed in 2015 by a calculation on two larger lattices with inverse lattice spacings of 1.730(4) GeV and 2.359(7) GeV and a continuum extrapolation performed [9]. We will focus on the latter calculation in this summary.

The calculation was performed using Möbius domain wall fermion (MDWF) ensembles of sizes $48^3 \times 96 \times 24$ (labeled 48I) and $64^3 \times 96 \times 12$ (labeled 64I), where the last dimension is the

extent of the fifth dimension, L_s. We used the Iwasaki gauge action with $\beta = 2.13$ and $\beta = 2.25$ for the 48I and 64I ensembles, respectively, and the Möbius scale was $\alpha = b + c = 2.0$ for both. More details on these ensembles can be found in Ref. [10].

In order to achieve physical kinematics we exploited the ability to modify the lattice boundary conditions (BCs) and used antiperiodic spatial BCs for the valence down quarks. As a result of this change, all charged pions become antiperiodic in each of the directions in which these BCs are applied, and their minimum allowed momentum in those directions rises from 0 (for periodic BCs) to $\pm\pi/L$ where L is the lattice size. By tuning L and the number of directions in which antiperiodic BCs are applied one can then match the ground-state energy of the two charged pion system to that of the kaon, such that the matrix element of interest becomes the ground-state contribution rather than an excited state. In order to take advantage of this we use the isospin symmetry to relate the $K^0 \to (\pi\pi)^{I=2}_{I_3=0}$ decay of interest to the unphysical amplitude $K^+ \to \pi^+\pi^+$ in which both pions are charged. This also allows us to ignore the fact that these BCs break the isospin symmetry; the $\pi^+\pi^+$ state is the only doubly-charged state in the system and is therefore prevented from mixing with other operators by charge conservation.

The renormalization was performed using the RI-SMOM($\not{q}, \not{q}$) and RI-SMOM(γ^μ, γ^μ) intermediate schemes [11] and the perturbative matching to the $\overline{\text{MS}}$ scheme peformed at 3 GeV. The RI-SMOM($\not{q}, \not{q}$) result was used for the central value and the other scheme was used to estimate the systematic error.

The results obtained for the real and imaginary components of the amplitude are

$$\text{Re}A_2 = 1.50(4)(14) \times 10^{-8} \text{ GeV} \tag{9}$$

$$\text{Im}A_2 = -6.99(20)(84) \times 10^{-14} \text{ GeV} \tag{10}$$

where the errors are statistical and systematic, respectively. The former is in good agreement with the experimental value of $\text{Re}A_2 = 1.4787(31) \times 10^{-8}$ GeV from charged kaon decays and $1.570(53) \times 10^{-8}$ GeV from neutral kaon decays.

As we can see above, the results are very precise for this amplitude, with $< 1\%$ statistical errors despite having performed a continuum extrapolation. The systematic error is much larger and is completely dominated by perturbative truncation errors in the NPR matching to $\overline{\text{MS}}$ (8%) and in the Wilson coefficients (12%). The latter is exacerbated by the fact that perturbation theory is being used to match the four and three-flavor theories across the charm threshold at 1.3 GeV where perturbation theory is less reliable.

4. The $\Delta I = 1/2$ rule

It has long been observed experimentally that the decay of the neutral kaon into an $I = 0$ final state is around 500× more likely than to an $I = 2$ state. This $\Delta I = 1/2$ rule is reflected in the ratio

$$\frac{1}{\omega} = \frac{\text{Re}A_0}{\text{Re}A_2} = 22.45(6), \tag{11}$$

the inverse of which enters directly as a coefficient in the determination of ϵ', Eq. 4. While around a factor of two in this ratio of amplitudes can be shown to arise from the perturbative running of

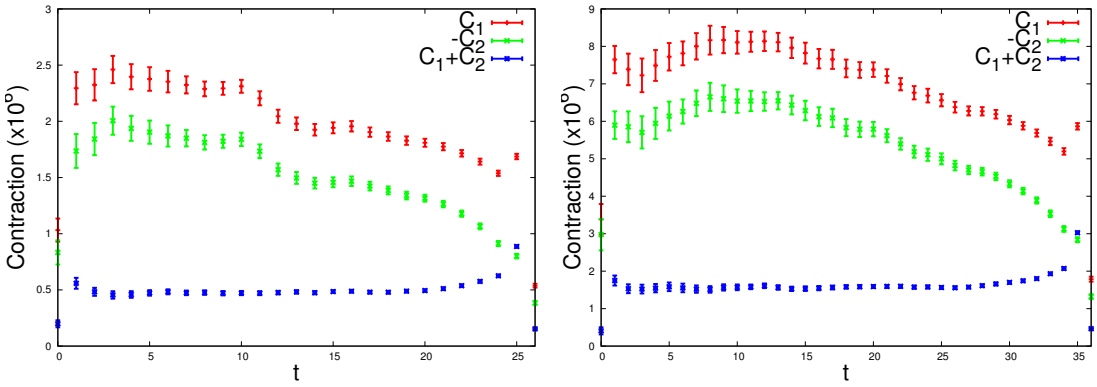

Figure 1: The two dominant contributions C_1 and C_2 to ReA_2 and their sum on the 48I (left) and 64I (right) ensembles, reproduced from Fig. 11 of Ref. [9].

the Wilson coefficients from the weak to the charm scale, the origin of the remaining factor of 10 has been a longstanding puzzle with no widely accepted explanation.

The $(27, 1)$ operator, which as mentioned above is the dominant contribution to Re(A_2), is computed on the lattice as the sum of two contractions C_1 and C_2. Naïve color counting suggests that $C_2 \approx 1/3\, C_1$, but in our calculation we found $C_2 \approx -0.7\, C_1$; i.e. they have opposite signs and nearly equal magnitudes. This results in a strong cancellation, illustrated in Fig. 1, that dramatically suppresses ReA_2. Note that this phenomenon is much less pronounced for simulations with heavier pions [18]. By combining our continuum result for ReA_2 with our latest determination of ReA_0 described below, we obtain

$$\frac{1}{\omega} = \frac{\mathrm{Re}A_0}{\mathrm{Re}A_2} = 19.9(5.0) \tag{12}$$

which is completely consistent with the experimental number. We therefore conclude that the $\Delta I = 1/2$ rule is a consequence of low-energy QCD.

5. First $I = 0$ calculation

The $I = 0$ amplitude receives contributions from all ten effective four-quark operators. The real part is dominated by the current-current operator Q_2 and the imaginary part by the QCD penguin operator Q_6 and to a lesser extent Q_4. The first calculation of the $I = 0$ amplitude was performed in 2015 [5] using a single lattice with essentially the same parameters as the ensemble used in the first calculation of A_2: We used 216 configurations of an MDWF ensemble of size $32^3 \times 64 \times 12$ with Möbius parameter $\alpha = b + c = 32/12$, physical pion masses and the Iwasaki+DSDR gauge action with $\beta = 1.75$ corresponding to an inverse lattice spacing of $a^{-1} = 1.378(7)$ GeV. Again this choice of lattice represents a compromise between having good control over residual finite-volume effects at the cost of increased discretization errors from the coarse lattice spacing, while maintaining a lattice size that is computationally feasible (significantly more statistics are needed for the A_0 calculation than the A_2 due to the disconnected diagrams).

To achieve physical kinematics for the ground-state matrix element we again exploit the lattice boundary conditions. Unfortunately, for the $I = 0$ case there is no way to avoid the isospin breaking introduced by imposing antiperiodic BCs on the down quark, nor is there a way to cast the problem

in terms of only charged pion states. Instead we utilize G-parity boundary conditions [12] in which the two light quark flavors undergo a charge conjugation and isospin rotation at the lattice spatial boundary. Both the charged and neutral pion states are negative eigenstates of the G-parity operation and the finite-volume action respects the isospin symmetry, hence when applied as a boundary condition we again achieve the raising of the ground-state pion momentum to $\pm\pi/L$ but for all pion states and without breaking isospin. This comes at a cost however: the Dirac operator in this setup is explicitly two-flavor, hence the computational cost of inverting the quark propagator is doubled; the fact that up-quark fermion operators can contract with down-quark antifermion operators and *vice versa* through a quark line that passes through the boundary adds significant complexity to the structure of the Wick contractions; and due to the presence of disconnected diagrams in the $I = 0$ case it is also necessary to generate custom ensembles with G-parity BCs on the sea quarks to avoid unitarity breaking effects. We used G-parity BCs in all three spatial directions resulting in a $\pi\pi$ ground-state energy that matches the kaon mass to within 2%.

The increased statistical errors induced by the disconnected diagrams were controlled through a combination of large statistics and by utilizing the all-to-all propagator framework [13] which allows for the convenient use of arbitrarily smeared operators – in our case $1s$ hydrogen wavefunction sources – whose properties can be tuned to maximize the overlap with the $\pi\pi$ state of interest and minimize the overlap with the vacuum. The two-pion source comprised two single-pion operators with back-to-back Fourier momentum of $(\pm1, \pm1, \pm1)\pi/L$ (with a total momentum of zero), and we averaged over all orientations to project onto the s-wave rotational state. The vacuum contribution was further reduced by separating the single-pion operators in the $\pi\pi$ source by 4 timeslices. We refer to this as the $\pi\pi(111)$ operator below.

The NPR was again performed using the RI-SMOM($\not{q}, \not{q}$) and RI-SMOM(γ^μ, γ^μ) intermediate schemes, with the former taken for the central value. In this case the matching to perturbation theory was performed at a lower scale of $\mu = 1.529$ GeV as necessitated by the lower lattice cutoff, thus increasing the perturbative truncation error relative to the A_2 case.

For this 2015 calculation we obtained the following results for the real and imaginary components of the amplitude,

$$\mathrm{Re}A_0 = 4.66(1.00)(1.26) \times 10^{-7} \ \text{GeV} \tag{13}$$

$$\mathrm{Im}A_0 = -1.90(1.23)(1.08) \times 10^{-11} \ \text{GeV}\,. \tag{14}$$

The former agrees with the experimental result of $\mathrm{Re}A_0 = 3.3201(18) \times 10^{-7}$ GeV. Here the much larger relative statistical error on the imaginary part is caused primarily by a large cancelation observed between the dominant Q_4 and Q_6 contributions. The systematic error is again dominated by perturbative truncation errors.

Combining the results for A_0 and A_2 we found

$$\mathrm{Re}(\epsilon'/\epsilon) = 1.38(5.15)(4.59) \times 10^{-4}, \tag{15}$$

which is 2.1σ below the experimental value, and the total error roughly $3\times$ the experimental error. It is clear that this is now a quantity that is accessible to lattice QCD, and our focus since that time has been on improving the statistics and better understanding our systematic errors.

6. The "$\pi\pi$ puzzle"

In order to reliably compute $K \to \pi\pi$ amplitudes on the lattice it is essential to have good control over the two-pion system. We measure $\pi\pi - \pi\pi$ two-point functions and from these extract the energies and the overlaps between our $\pi\pi$ operators and the ground and excited $\pi\pi$ states, both of which are used directly to extract the matrix element from the $K \to \pi\pi$ three-point functions. The ground-state energy is also used to compute the $\pi\pi$ phase shift using the Lüscher prescription [14], which is required to obtain ϵ' via Eq. (4). In the 2015 calculation we obtained a value of $\delta_0(E_{\pi\pi} \approx m_K) = 23.8(4.9)(1.2)^\circ$ which is substantially smaller than the prediction of $\sim 39^\circ$ obtained by combining the dispersive Roy equations with experimental input [15].

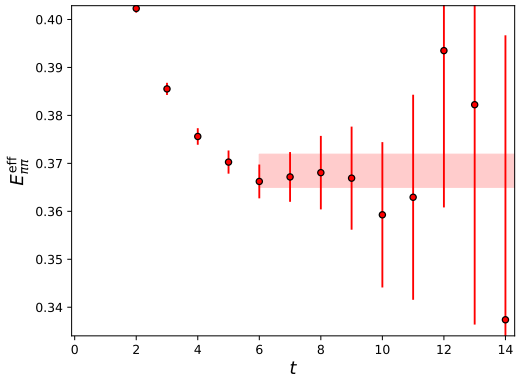

Figure 2: The $\pi\pi$ effective energy obtained using 1438 configurations with the $\pi\pi(111)$ operator.

In order to better understand this discrepancy, following the 2015 calculation we dramatically increased our statistics from 216 to 1438 configurations, but rather than improving the agreement we found an even lower value of $19.1(2.5)^\circ$ [16]. The effective mass plot for this $\pi\pi$ two-point function is shown in Fig. 2. While this result was stable under varying the fit ranges and also with two-state fits, the rapid error growth visible in the figure suggests that the most likely origin of the discrepancy is due to nearby excited states whose presence is masked by the rapid degeneration of the signal. To resolve this issue we expanded our two-pion operator basis, incorporating two additional $\pi\pi$ operators: the $\pi\pi(311)$ operator in which the two constituent pions are again moving back-to-back as in the $\pi\pi(111)$ case, but here with the next allowed momenta $(\pm 3, \pm 1, \pm 1)\pi/L$ and permutations thereof; and the scalar $\sigma = \frac{1}{\sqrt{2}}(\bar{u}u + \bar{d}d)$ operator, which also has vacuum quantum numbers and thus projects onto the $I = 0$ $\pi\pi$ state. By varying the source and sink operator we are then able to construct a 3×3 (symmetric) matrix of correlation functions that can be fit simultaneously to determine the energies of multiple states and the overlaps of the operators with those states. As we will demonstrate below, this technique is much more powerful than merely fitting the large time dependence of the two-point functions from a single operator.

Using the three $\pi\pi$ operators detailed above we repeated our calculation of A_0 on 741 configurations of the same ensemble [1]. In Fig. 3 we show the result for the $\pi\pi$ ground-state energy obtained by varying the fit range, the number of operators and the number of states in the $\pi\pi$ two-point function fits. The 1-operator, 1-state result in this figure is equivalent to the fits performed

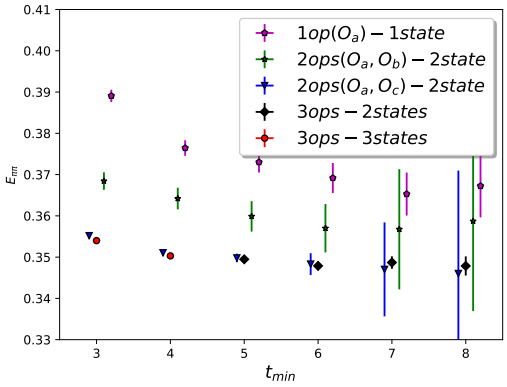

Figure 3: The $I = 0$ $\pi\pi$ energy obtained by varying the lower bound on the fit range t_{min}, the number of operators and number of states. In the legend O_a, O_b, O_c correspond to the $\pi\pi(111)$, $\pi\pi(311)$ and σ operators, respectively. Our best fit is the 3-operator, 2-state result with $t_{\text{min}} = 6$.

in our 2015 calculation, and again we see an apparent plateau at $t_{\text{min}} = 6$ or 7; however in adding further operators we see a marked shift in the fitted energy to lower values as well as a dramatic improvement in the quality of the plateau and the statistical error, thus demonstrating the presence of excited state contamination. This figure also exemplifies the power of the multi-operator technique, providing a much larger reduction in the statistical error than would be obtained for the same cost merely by increasing statistics. For our final result we obtained

$$\delta_0(471 \text{ MeV}) = 32.3(1.0)(1.4)^\circ . \tag{16}$$

This result is in much better agreement with the dispersive prediction at this energy of 35.9°, hence we conclude that the discrepancy with the dispersive result was indeed due to excited state contamination and that the issue has now been resolved. For more details on the fits to the two-point functions and our procedures for estimating the systematic errors, as well as an expansion of the phase shift determination to moving-frame $\pi\pi$ operators with lower center of mass energies, we direct the reader to our companion paper, Ref. [16]. Note that the result above is reproduced from Ref. [16] and has a systematic error that differs slightly from the earlier result given in Ref. [1]; this difference is sufficiently small that it has no significant impact on the determination of ϵ'.

7. Improved determination of A_0

The $K \to \pi\pi$ matrix elements are obtained by fitting to three-point functions of the form

$$C_i(t, t_{\text{sep}}^{K\to\text{snk}}) = \langle 0|O_{\text{snk}}^{\dagger}(t_{\text{sep}}^{K\to\text{snk}})Q_i(t)O_K(0)|0\rangle \tag{17}$$

where O_K is the kaon operator, O_{snk} one of the $\pi\pi$ operators and Q_i are the (subtracted) weak effective operators. We measured with five different source-sink separations $t_{\text{sep}}^{K\to\text{snk}} \in \{10, 12, 14, 16, 18\}$ and Q_i is inserted on all intervening timeslices. We simultaneously fit over all $t_{\text{sep}}^{K\to\text{snk}}$ and choice of O_{snk}, and apply cuts on the minimum time separation t_{min} between the kaon and the four-quark operator, as well as the minimum time separation t'_{min} between the four-quark operator and the $\pi\pi$

sink, where $t' = t_{\text{sep}}^{K\to\text{snk}} - t$. For this improved calculation we also use 741 configurations of the same ensemble used in our 2015 calculation.

For plotting purposes we define an effective $K \to \pi\pi$ matrix element,

$$\begin{aligned} M_i^{\text{eff,snk}}(t') &= C_i(t, t_{\text{sep}}^{K\to\text{snk}}) \left(\frac{1}{\sqrt{2}} A_K A_{\text{snk}}^0 e^{-m_K t} e^{-E_0(t_{\text{sep}}^{K\to\text{snk}} - t)} \right)^{-1} \\ &= M_i^0 + \sum_j \frac{A_{\text{snk}}^j}{A_{\text{snk}}^0} M_i^j e^{-(E_j - E_0)t'} \,. \end{aligned} \tag{18}$$

where A_K and m_K are the ground-state kaon operator-overlap coefficient and mass, respectively, and A_{snk}^j and E_j are the operator-overlap and energy of the $\pi\pi$ ground and excited states. These results are obtained from their respective two-point function fits. We apply a uniform cut of $t_{\text{min}} = 6$ to ensure that only the kaon ground state contributes. These effective matrix elements converge to the desired matrix elements M_i^0 at large t'.

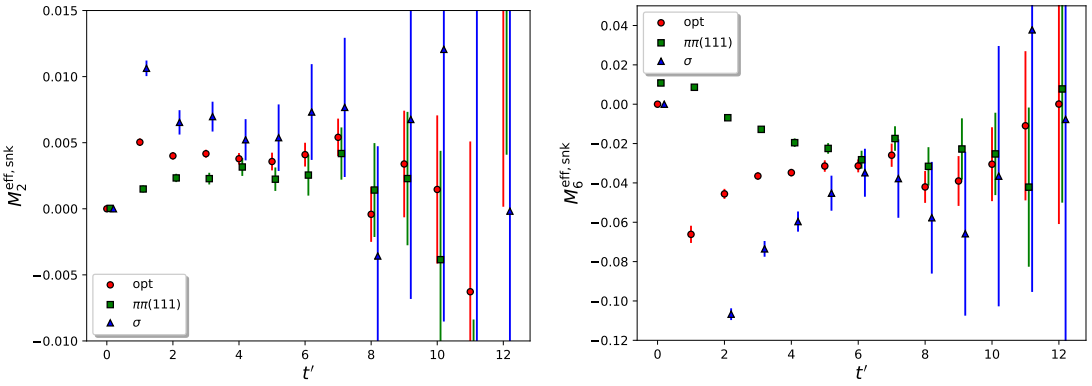

Figure 4: The effective matrix elements of the Q_2 and Q_6 operators for the $\pi\pi(111)$, σ and optimal operators as a function of the time separation t' between the four-quark operator and the $\pi\pi$ sink operator.

In order to demonstrate the effect of the additional $\pi\pi$ operators on the matrix elements we further define an optimal operator $O_{\text{opt}} = \sum_i r_i O_{\text{snk},i}$ where r_i are chosen based on the results of the $\pi\pi$ two-point function fits to maximize the overlap of this operator with the ground state. For our best fit with three operators and two states, this correlator matrix is not square hence there is no unique definition of r_i; however Fig. 3 shows that the vast majority of the improvement is obtained from just the $\pi\pi(111)$ and σ operators. We therefore compute r_i from the 2×2 correlator matrix with these operators and two states. In Fig. 4 we show the effective matrix elements of Q_2 and Q_6, which are the dominant contributions to the real and imaginary parts of A_0, respectively, for the $\pi\pi(111)$, σ and optimal sink operators. As we saw for the $\pi\pi$ fits, the introduction of more operators results in a clear and marked improvement in both the statistical errors and on the quality of the plateau.

We varied the number of operators, states and the temporal cuts in order to probe the excited state errors and to obtain our best fit. In Fig. 5 we plot the results of those fits. In the Q_2 case we find good agreement between all of the fits for $t'_{\text{min}} \geq 4$, although we see improved statistical errors with the additional operators. However for Q_6 we see a clear pattern of excited state contamination in

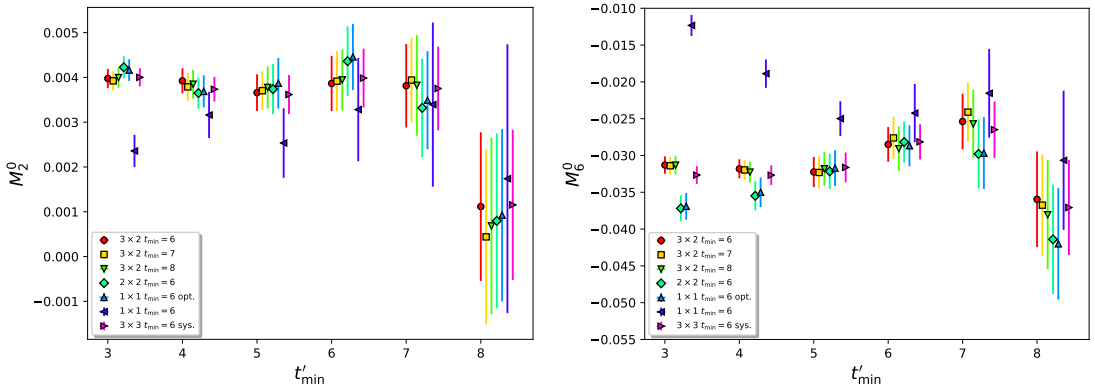

Figure 5: The fitted ground-state matrix elements of the Q_2 and Q_6 operators for various choices of the number of operators, number of states and the cut t_{min} between the kaon and four-quark operators, as a function of the cut t'_{min} between the four-quark operator and the $\pi\pi$ sink. In the legend "$a \times b$" indicates the fit was performed with a operators and b states, and "opt." indicates the optimal operator was used. In the two-operator case we drop the $\pi\pi(311)$ operator and in the one-operator case we further drop the σ. The "sys." results are obtained using three operators and three states for both the $\pi\pi$ and $K \to \pi\pi$ fits and is used in the systematic error estimation. The values are shifted for clarity.

the one and two-operator fit results, the latter converging later than the former as we would expect. The final best fit for all operators was obtained with three operators and two states with $t'_{\text{min}} = 5$ and $t_{\text{min}} = 6$. The best fit from the 2015 calculation would correspond here to the "1×1 $t_{\text{min}} = 6$" point with $t'_{\text{min}} = 4$, which we see is very different from our new best fit; unfortunately this implies that our $\leq 5\%$ estimate for the excited state contamination in our 2015 calculation was significantly underestimated.

Alongside the additional $\pi\pi$ operators, another significant improvement in this updated calculation is the use of step-scaling [17] to circumvent the limit imposed by the coarse lattice spacing on the largest renormalization scale that can be used for the NPR. This procedure involves computing the step-scaling matrix

$$\Lambda^{\text{RI}}(\mu_2, \mu_1) = Z^{\text{RI}\leftarrow\text{lat}}(\mu_2) \left[Z^{\text{RI}\leftarrow\text{lat}}(\mu_1)\right]^{-1} \tag{19}$$

on a finer ensemble, where μ_1 is a scale accessible to the coarse ensemble, $\mu_2 > \mu_1$ is a scale accessible to the fine ensemble, and $Z^{\text{RI}\leftarrow\text{lat}}(\mu)$ is the RI-SMOM NPR matrix. Λ^{RI} therefore encapsulates the non-perturbative running of the renormalization factor, and has a well defined continuum limit. In principle this continuum limit should be taken to remove discretization errors on Λ^{RI} but these effects are small and can be neglected assuming it is computed on a fine enough lattice. We then compute $Z^{\text{RI}\leftarrow\text{lat}}(\mu_1)$ on the coarse ensemble and apply Λ^{RI} to raise the renormalization scale,

$$Z^{\text{RI}\leftarrow\text{lat}}(\mu_2) = \Lambda^{\text{RI}}(\mu_2, \mu_1) Z^{\text{RI}\leftarrow\text{lat}}(\mu_1)\,. \tag{20}$$

For this calculation we used the "32Ifine" ensemble described in Ref. [10], which has $a^{-1} = 3.148(17)$ GeV, and used $\mu_2 = 4.006$ GeV and $\mu_1 = 1.53$ GeV. As we will show below, the adoption of this higher scale resulted in a factor of three reduction in our NPR systematic error.

8. New results for A_0 and ϵ'

For our new calculation we find [1]

$$\mathrm{Re}A_0 = 2.99(0.32)(0.59) \times 10^{-7} \text{ GeV} \tag{21}$$

$$\mathrm{Im}A_0 = -6.98(0.62)(1.44) \times 10^{-11} \text{ GeV} \tag{22}$$

The former agrees well with the experimental result $\mathrm{Re}A_0 = 3.3201(18) \times 10^{-7}$ GeV and with our previous result. The value for $\mathrm{Im}A_0$ differs substantially however, which gives rise to a similarly large change in ϵ':

$$\mathrm{Re}(\epsilon'/\epsilon) = 21.7(2.6)(6.2)(5.0) \times 10^{-4}, \tag{23}$$

which is now in good agreement with the experimental number. In Ref. [1] we perform a detailed study of the origin of the difference between our new and old calculations and determine that it is primarily driven by the excited state contamination discussed in the previous section, which is removed by introducing additional operators and increasing t'_{min} from 4 to 5.

We now discuss the systematic error budget. The third set of parentheses in Eq. 23 gives an estimate of the effects of isospin breaking (IB) and electromagnetism (EM), which for ϵ' are significantly enhanced over their typical percent-scale size because of the 20× suppression of A_2 by the mechanics of the $\Delta I = 1/2$ rule increasing the relative effect of EM+IB on this term. This 23% systematic error is the largest single contribution to our budget and is presently estimated using next-to-leading order chiral perturbation theory with some input from the $1/N_c$ expansion [19].

A detailed discussion of the remaining systematic errors and their estimation can be found in Ref. [1]. Below we focus on the dominant systematic errors of the 2015 calculation and describe how they have changed in our updated result:

- The discretization error resulting primarily from the use of a single, somewhat coarse $a^{-1} = 1.38$ GeV lattice spacing in the determination of A_0. We estimate 12% for this error based on the continuum extrapolation behavior of the $\Delta I = 3/2$ operators, and this remains unchanged from our 2015 calculation.

- The error on the perturbative Wilson coefficients. For the 2015 calculation we estimated 12% for this error by comparing the results with leading and next-to-leading order perturbation theory. In the new calculation we might have hoped that raising the RI $\to \overline{\mathrm{MS}}$ matching scale from 1.53 GeV to 4 GeV would improve this error, but in fact we have deduced that the bulk of the error arises from the use of perturbation theory to match the 3- and 4-flavor theories across the charm threshold, which is performed at $m_c \approx 1.3$ GeV before running up to 4 GeV in the 3-flavor theory. Thus we continue to estimate a 12% contribution for this source of error.

- The error on the NPR resulting from using perturbation theory to match between the RI and $\overline{\mathrm{MS}}$ schemes. By studying the behavior of the difference between the results obtained with the RI-SMOM($\not{q}, \not{q}$) and RI-SMOM(γ^μ, γ^μ) intermediate schemes as a function of the matching scale, we conclude that this error has reduced from 15% on our 2015 calculation to just 5% as a result of using step-scaling to increase the matching scale to 4 GeV.

- The error on the Lellouch-Lüscher factor F arising from the uncertainty in the derivative of the $I = 0$ $\pi\pi$ phase shift as a function of energy. Due to our greatly improved understanding and confidence in the behavior of the $\pi\pi$ system, and the fact that we are able to independently compute this derivative purely from the lattice (albeit with somewhat large errors), we reduced this systematic error from 12% to 1.5%. The reader should note that the above derivative is a subdominant contribution to F with the majority arising from a known analytic function, hence this 1.5% error actually arises from a 12% variation in the derivative.

- Excited state contamination in the $I = 0$ $K \to \pi\pi$ and $\pi\pi - \pi\pi$ correlation function fits. In the 2015 calculation, owing the to the stability of the fits and the clear apparent plateau, we assigned a $\leq 5\%$ error to this source. However, as we have described above, this error was significantly underestimated. By introducing more $\pi\pi$ operators and increasing statistics we have obtained much more reliable results and conclude that the excited state contamination is now negligible in comparison to our other error sources.

9. Outlook

Since the publication of the updated calculation we have started preparing for future calculations to further improve statistics and address our remaining systematic errors. The most important are the effects of isospin breaking and electromagnetism, which together contribute our dominant systematic error and for which the uncertainty may be large due to the reliance on chiral perturbation theory and the $1/N_c$ expansion. Unfortunately, significant theoretical and computational hurdles must be overcome before a lattice calculation of these effects becomes possible, primarily related to the treatment of the long-range electromagnetic interactions in a finite box. A popular technique, QED_L, allows for the treatment of QED on the lattice by explicitly removing the zero modes from the photon propagator, at the cost of introducing new $1/L$ power-law finite-volume corrections that must be determined. We are investigating [20] an alternate technique whereby Coulomb gauge is used to separate the QED interaction into a static Coulomb potential component and a component involving only transverse photons. The static potential is truncated to a finite range R and placed on the lattice, incurring $1/R$ corrections that can be computed analytically using infinite volume perturbation theory. Additional work will be required to include the transverse photon contributions. A potential difficulty for application to $K \to \pi\pi$ is the fact that these QED approaches are not clearly compatible with G-parity boundary conditions where the boundary changes up into down quarks and *vice versa*, thus breaking charge conservation.

Another significant systematic error arises due to the use of perturbation theory to match across the charm threshold between the four flavor theory and the three flavor theory in which we simulate the decay. This can be circumvented by performing a simulation in the four-flavor theory directly, but the combined requirement of fine lattice spacings to control charm discretization effects and large physical volumes to control finite volume errors puts this out of the reach of the present generation of supercomputers. We are investigating an alternative approach [21, 22] whereby the Wilson coefficients relating the three and four flavor theories are computed non-perturbatively by evaluating suitable ratios of renormalized Green's functions containing the three and four-flavor weak effective operators on the same three flavor lattice (i.e. neglecting charm sea effects) at

energies much below the charm quark mass, $\mu \ll m_c$. One of the major difficulties of this calculation is in finding a renormalization scheme suitable for evaluation at such low energy scales; in this regime the RI-SMOM schemes tend to become very noisy and mixing occurs with a tower of gauge-noninvariant operators entering due to the reliance on gauge fixing. For this calculation we are investigating the use of position-space renormalization techniques which do not require gauge fixing.

The most significant pure-lattice systematic error is due to the determination of A_0 on only a single, rather coarse ensemble. We estimated the size of these effects by studying the scaling dependence of the three operators entering the $I = 2$ amplitude, for which continuum results are available. However it is not clear the extent to which this estimate is reliable due to the different physics pertaining to the $I = 0$ amplitude. To address this issue we are proceeding down two complementary avenues. The dramatic impact of the multiple operator technique for isolating the physical $K \to \pi\pi$ matrix element from the contributions of nearby $\pi\pi$ states has reopened the question of whether it is possible to perform a similarly precise calculation of A_0 using regular periodic boundary conditions rather than G-parity BCs. This offers a number of advantages such as not requiring the generation of custom ensembles, a factor of two lower computational cost in evaluating quark propagators and a significant amount of computational effort (such as the determination of eigenvectors) can be shared with other projects, at the cost of the physical matrix element becoming a subdominant contribution to the three-point Green's functions. It also serves as a valuable cross-check of our G-parity result. We are presently performing an exploratory calculation on two ensembles [23], the first the $32^3 \times 64$ domain wall fermion ensemble with physical pion masses, periodic BCs and $a^{-1} \approx 1.4$ GeV that was used for our original calculation of A_2 [7, 8] (our current calculation of A_0 is performed on a lattice with the same parameters and G-parity BCs) and the second a coarser $24^3 \times 64$ ensemble with $a^{-1} \approx 1$ GeV.

We are also looking to leverage the computational power of the new generation of supercomputers presently coming online to directly extend our G-parity calculation with additional lattice spacings. To this end we have developed code using the Grid [24, 25] library to perform gauge field generation with G-parity boundary conditions that is optimized for calculation on GPUs, and have commenced the generation of two new ensembles on the Perlmutter machine: a $40^3 \times 64$ lattice with $a^{-1} \approx 1.7$ GeV and a $48^3 \times 64$ lattice with $a^{-1} \approx 2.1$ GeV. The parameters of these ensembles were carefully chosen to maintain the same physical volume – and hence $\pi\pi$ energy – as our present calculation, thus ensuring a physical decay. Like our existing calculation, both of these ensembles use Möbius DWF for which discretization effects enter at $O(a^2)$ and higher, hence we will obtain a factor of two lever arm in the a^2 continuum extrapolation with a third intermediate point to demonstrate linear scaling.

10. Conclusions

We have completed an update to our 2015 calculation of the measure of direct CP-violation in $K \to \pi\pi$ decays, ϵ', with $2\times$ smaller statistical errors and more robust and reliable systematic errors. Notably we have achieved much greater control over errors resulting from the contribution of nearby $\pi\pi$ excited states in our matrix element fits by including multiple $\pi\pi$ operators in a simultaneous fit to more reliably extract the ground-state dependence, and have reduced the systematic error

arising from the truncation of the perturbative series used in matching our non-perturbative lattice renormalization scheme to the $\overline{\text{MS}}$ by a factor of three using step-scaling. We obtain a result that is in good agreement with the experimental value and a total error ∼3.6× that of the experiment. We also perform an *ab initio* computation of the ratio $\text{Re}A_0/\text{Im}A_2$ which is compatible with the experimental value, thus explaining the decades-old puzzle of the origin of the $\Delta I = 1/2$ rule enhancement of this quantity as a consequence of non-perturbative QCD.

We believe that ϵ' remains a promising avenue in which to search for new physics, and we have detailed in this document our ongoing plans and ambitions to achieve an increased precision which may reveal these effects.

References

[1] R. Abbott *et al.* [RBC and UKQCD], Phys. Rev. D **102**, no.5, 054509 (2020) doi:10.1103/PhysRevD.102.054509 [arXiv:2004.09440 [hep-lat]].

[2] J. R. Batley *et al.* [NA48], Phys. Lett. B **544**, 97-112 (2002) doi:10.1016/S0370-2693(02)02476-0 [arXiv:hep-ex/0208009 [hep-ex]].

[3] E. Abouzaid *et al.* [KTeV], Phys. Rev. D **83**, 092001 (2011) doi:10.1103/PhysRevD.83.092001 [arXiv:1011.0127 [hep-ex]].

[4] M. Tanabashi *et al.* [Particle Data Group], Phys. Rev. D **98**, no.3, 030001 (2018) doi:10.1103/PhysRevD.98.030001

[5] Z. Bai *et al.* [RBC and UKQCD], Phys. Rev. Lett. **115**, no.21, 212001 (2015) doi:10.1103/PhysRevLett.115.212001 [arXiv:1505.07863 [hep-lat]].

[6] L. Lellouch and M. Luscher, Commun. Math. Phys. **219**, 31-44 (2001) doi:10.1007/s002200100410 [arXiv:hep-lat/0003023 [hep-lat]].

[7] T. Blum, P. A. Boyle, N. H. Christ, N. Garron, E. Goode, T. Izubuchi, C. Jung, C. Kelly, C. Lehner and M. Lightman, *et al.* Phys. Rev. Lett. **108**, 141601 (2012) doi:10.1103/PhysRevLett.108.141601 [arXiv:1111.1699 [hep-lat]].

[8] T. Blum, P. A. Boyle, N. H. Christ, N. Garron, E. Goode, T. Izubuchi, C. Jung, C. Kelly, C. Lehner and M. Lightman, *et al.* Phys. Rev. D **86**, 074513 (2012) doi:10.1103/PhysRevD.86.074513 [arXiv:1206.5142 [hep-lat]].

[9] T. Blum, P. A. Boyle, N. H. Christ, J. Frison, N. Garron, T. Janowski, C. Jung, C. Kelly, C. Lehner and A. Lytle, *et al.* Phys. Rev. D **91**, no.7, 074502 (2015) doi:10.1103/PhysRevD.91.074502 [arXiv:1502.00263 [hep-lat]].

[10] T. Blum *et al.* [RBC and UKQCD], Phys. Rev. D **93**, no.7, 074505 (2016) doi:10.1103/PhysRevD.93.074505 [arXiv:1411.7017 [hep-lat]].

[11] C. Sturm, Y. Aoki, N. H. Christ, T. Izubuchi, C. T. C. Sachrajda and A. Soni, Phys. Rev. D **80**, 014501 (2009) doi:10.1103/PhysRevD.80.014501 [arXiv:0901.2599 [hep-ph]].

[12] N. H. Christ, C. Kelly and D. Zhang, Phys. Rev. D **101**, no.1, 014506 (2020) doi:10.1103/PhysRevD.101.014506 [arXiv:1908.08640 [hep-lat]].

[13] J. Foley, K. Jimmy Juge, A. O'Cais, M. Peardon, S. M. Ryan and J. I. Skullerud, Comput. Phys. Commun. **172**, 145-162 (2005) doi:10.1016/j.cpc.2005.06.008 [arXiv:hep-lat/0505023 [hep-lat]].

[14] M. Luscher, Nucl. Phys. B **354**, 531-578 (1991) doi:10.1016/0550-3213(91)90366-6

[15] G. Colangelo, J. Gasser and H. Leutwyler, Nucl. Phys. B **603**, 125-179 (2001) doi:10.1016/S0550-3213(01)00147-X [arXiv:hep-ph/0103088 [hep-ph]].

[16] T. Blum *et al.* [RBC and UKQCD], [arXiv:2103.15131 [hep-lat]].

[17] R. Arthur *et al.* [RBC and UKQCD], Phys. Rev. D **83**, 114511 (2011) doi:10.1103/PhysRevD.83.114511 [arXiv:1006.0422 [hep-lat]].

[18] P. A. Boyle *et al.* [RBC and UKQCD], Phys. Rev. Lett. **110**, no.15, 152001 (2013) doi:10.1103/PhysRevLett.110.152001 [arXiv:1212.1474 [hep-lat]].

[19] V. Cirigliano, H. Gisbert, A. Pich and A. Rodríguez-Sánchez, JHEP **02**, 032 (2020) doi:10.1007/JHEP02(2020)032 [arXiv:1911.01359 [hep-ph]].

[20] J. Karpie, PoS **LATTICE2021**, 312 (2021)

[21] M. Tomii, PoS **LATTICE2018**, 216 (2019) doi:10.22323/1.334.0216 [arXiv:1901.04107 [hep-lat]].

[22] M. Tomii, PoS **LATTICE2019**, 174 (2020) doi:10.22323/1.363.0174

[23] M. Tomii, PoS **LATTICE2021**, 394 (2021)

[24] P. Boyle, A. Yamaguchi, G. Cossu and A. Portelli, [arXiv:1512.03487 [hep-lat]].

[25] P. A. Boyle, M. A. Clark, C. DeTar, M. Lin, V. Rana and A. V. Avilés-Casco, EPJ Web Conf. **175**, 09006 (2018) doi:10.1051/epjconf/201817509006 [arXiv:1710.09409 [hep-lat]].